Molecular Pharmacology Fast Forward. Published on March 18, 2014 as doi:10.1124/mol.113.091272
This article has not been copyedited and formatted. The final version may differ from this version.

Sensory nerve terminal mitochondrial dysfunction induces hyperexcitability in airway nociceptors via protein kinase C

Stephen H Hadley, Parmvir K Bahia, Thomas E Taylor-Clark

Department of Molecular Pharmacology & Physiology, College of Medicine, University of South Florida, Tampa, Florida, USA.

Molecular Pharmacology Fast Forward. Published on March 18, 2014 as DOI: 10.1124/mol.113.091272
This article has not been copyedited and formatted. The final version may differ from this version.

Running title: Mitochondrial ROS induces hyperexcitability

***Corresponding Author:** Thomas Taylor-Clark

ttaylorc@health.usf.edu

12901 Bruce B Downs Blvd, University of South Florida, Tampa, FL, 33612

813-974-7749 (t), 813-974-3079 (f)

Number of text pages: 36

Number of tables: 0

Number of Figures: 6

Number of References: 58

Word Count Abstract: 249

Word Count Introduction: 514

Word Count Discussion: 1495

Abbreviations: α,β mATP, α,β methylene ATP; AITC, allyl isothiocyanate; BIM, bisindolylmaleimide; CV, conduction velocity; DAG, diacylglycerol; DRG, dorsal root ganglion; DTT, dithiothreitol; GSH, glutathione; I-RTX, 5'-Iodoresiniferatoxin; NAC, N-acetylcysteine; PKC, protein kinase C; PMA, phorbol-12-myristate-13-acetate; ROS, reactive oxygen species; TRPA1, transient receptor potential ankyrin 1; TRPV1, transient receptor potential vanilloid 1.

Molecular Pharmacology Fast Forward. Published on March 18, 2014 as DOI: 10.1124/mol.113.091272
This article has not been copyedited and formatted. The final version may differ from this version.

ABSTRACT

Airway sensory nerve excitability is a key determinant of respiratory disease-associated reflexes and sensations such as cough and dyspnea. Inflammatory signaling modulates mitochondrial function and produces reactive oxygen species (ROS). Peripheral terminals of sensory nerves are densely packed with mitochondria, thus we hypothesized that mitochondrial modulation would alter neuronal excitability. We recorded action potential firing from the terminals of individual bronchopulmonary C-fibers using a mouse ex vivo lung-vagal ganglia preparation. C-fibers were characterized as nociceptors or non-nociceptors based upon conduction velocity and response to transient receptor potential (TRP) channel agonists. Antimycin A (mitochondrial complex III Q_i site inhibitor) had no effect on the excitability of non-nociceptors. However, antimycin A increased excitability in nociceptive C-fibers: decreasing the mechanical threshold by 50% and increasing the action potential firing elicited by a $P2X_{2/3}$ agonist to 270% of control. Antimycin A-induced nociceptor hyperexcitability was independent of TRP ankyrin 1 (TRPA1) or TRP vanilloid 1 (TRPV1) channels. Blocking mitochondrial ATP production with oligomycin or myxothiazol had no effect on excitability. Antimycin A-induced hyperexcitability was dependent on mitochondrial ROS and was blocked by intracellular antioxidants. ROS are known to activate protein kinase C (PKC). Antimycin A-induced hyperexcitability was inhibited by the PKC inhibitor bisindolylmaleimide (BIM) I, but not by its inactive analogue BIM V. In dissociated vagal neurons antimycin A caused ROS-dependent PKC translocation to the membrane. Finally, H_2O_2 also induced PKC-dependent nociceptive C-fiber hyperexcitability and PKC translocation. In conclusion, ROS evoked by mitochondrial dysfunction caused nociceptor hyperexcitability via the translocation and activation of PKC.

Molecular Pharmacology Fast Forward. Published on March 18, 2014 as DOI: 10.1124/mol.113.091272
This article has not been copyedited and formatted. The final version may differ from this version.

INTRODUCTION

A large subset of sensory nerves in the somatosensory and visceral systems are “nociceptive”: they are adapted to detect noxious and potential noxious stimuli and then trigger sensations, behaviors and reflexes that are intended to diminish future noxious threats. Nevertheless nociceptor excitability is not static and in damaged and inflamed tissues nociceptors can become hyperexcitable such that sub-threshold stimuli inappropriately evoke nociceptive responses or that super-threshold stimuli evoke inappropriately large responses. The bronchopulmonary airways are densely innervated by nociceptive vagal C-fibers, whose activation leads to the initiation of reflexes (cough, hypersecretion, bronchospasm) and sensations (dyspnea, itch, urge to cough) (Carr and Undem, 2003). Airway nociceptive reflexes are exacerbated in inflammatory and infectious airway disease (Carr and Lee, 2005; Nassenstein et al., 2007; Riccio et al., 1996; Sabogal et al., 2005), most clearly observed clinically as an excessive and hyperresponsive cough in respiratory disease (Jesenak et al., 2009; Morice, 2010). As such there is considerable interest in understanding the mechanisms through which inflammation and other noxious stimuli modulate nociceptor excitability.

Increasing evidence suggests that mitochondrial dysfunction contributes to inflammation in multiple tissues via the actions of mitochondrially-evoked reactive oxygen species (ROS) (Reddy, 2011; Sena and Chandel, 2012). DNA mutations leading to aberrant mitochondrial protein function/expression have been known for many years to dramatically impact ATP production and ROS signaling. Recently it was shown that numerous signaling events can also increase mitochondrial ROS production, e.g. hypoxia (Bell et al., 2007), TNFα (Corda et al., 2001), neurotrophins via p75NTR (Pehar et al., 2007), TGFβ (Michaeloudes et al., 2010) and

Molecular Pharmacology Fast Forward. Published on March 18, 2014 as DOI: 10.1124/mol.113.091272
This article has not been copyedited and formatted. The final version may differ from this version.

Toll-like Receptors (West et al., 2011). This is likely of particular importance for the peripheral terminals of sensory nerves, which contain a high density of mitochondria (Hung et al., 1973; von During and Andres, 1988). We have previously shown an interaction between nerve terminal mitochondria and nerve terminal function in a study that demonstrated that mitochondrial ROS can cause overt bronchopulmonary C-fiber activation (action potential discharge) via the selective gating of transient receptor potential ankyrin 1 (TRPA1) (Nesuashvili et al., 2013). It is not yet known if mitochondrial ROS can also modulate neuronal excitability.

To study the effect of mitochondrial dysfunction and ROS on bronchopulmonary C-fiber excitability we have used antimycin A, a selective inhibitor of the Q_i site on complex III in the mitochondrial electron transport chain. This selective inhibitor stimulates mitochondrial superoxide formation and the subsequent production of numerous ROS (Gyulkhandanyan and Pennefather, 2004; Stowe and Camara, 2009; Tretter et al., 2007; Turrens et al., 1985). Cellular oxidation can modulate the function of numerous proteins, including ion channels and enzymes (Stowe and Camara, 2009; Thannickal and Fanburg, 2000). In particular protein kinase C (PKC) can be activated by ROS independently of Ca^{2+} or diacylglycerol (DAG) (Gopalakrishna and Anderson, 1989; Knapp and Klann, 2000). PKC activation is known to induce nociceptor hyperexcitability in somatosensory neurons via its phosphorylation of voltage-gated and ligand-gated ion channels (Amadesi et al., 2004; Baker, 2005; Cesare et al., 1999; Wu et al., 2012). Here, we found that mitochondrial ROS induced hyperexcitability of nociceptive bronchopulmonary C-fibers via oxidative activation and translocation of PKC.

Molecular Pharmacology Fast Forward. Published on March 18, 2014 as DOI: 10.1124/mol.113.091272
This article has not been copyedited and formatted. The final version may differ from this version.

MATERIALS AND METHODS

All experiments were approved by the University of South Florida Institutional Animal Care and Use Committee.

Bronchopulmonary C-fiber extracellular recordings: Male C57BL/6J mice (Jackson Laboratory, Maine) were killed by CO_2 asphyxiation followed by exsanguination. The innervated isolated lung preparation was prepared as previously described (Nassenstein et al., 2008; Nesuashvili et al., 2013). Briefly, the airways and lungs with their intact extrinsic innervation (vagus nerve including vagal ganglia) were taken and placed in a dissecting dish containing Krebs bicarbonate buffer solution composed of (mM): 118 NaCl, 5.4 KCl, 1.0 NaH_2PO_4, 1.2 $MgSO_4$, 1.9 $CaCl_2$, 25.0 $NaHCO_3$ and 11.1 D-glucose, and equilibrated with 95% O_2 and 5% CO_2 (pH 7.3–7.4) and containing 3 μM indomethacin. Connective tissue was trimmed away leaving the trachea and lungs with their intact nerves. The airways were then pinned to the larger compartment of a custom-built two-compartment recording chamber that was lined with silicone elastomer (Sylgard). A vagal ganglion was pulled into the adjacent compartment of the chamber through a small hole and pinned. Both compartments were separately superfused with Krebs bicarbonate buffer (37°C). A sharp glass electrode was pulled by a Flaming Brown micropipette puller (P-87; Sutter Instruments, Novato, CA, USA) and filled with 3 M NaCl solution. The electrode was inserted and placed near the cell bodies of vagal ganglion. The recorded action potentials were amplified (Microelectrode AC amplifier 1800; A-M Systems, Everett, WA, USA), filtered (0.3 kHz of low cut-off and 1 kHz of high cut-off), and monitored on an oscilloscope (TDS1002B; Tektronix, Beaverton, OR, USA). The scaled output from the amplifier was captured and analyzed by a Macintosh computer using NerveOfIt software

Molecular Pharmacology Fast Forward. Published on March 18, 2014 as DOI: 10.1124/mol.113.091272
This article has not been copyedited and formatted. The final version may differ from this version.

(Phocis, Baltimore, MD, USA). Action potential discharge was quantified off-line and recorded in 1 s bins. The background activity was usually either absent or less than 2 Hz.

Nerve fiber characterization: To measure conduction velocity, an electrical stimulation (S44; Grass Instruments, Quincy, MA, USA) was applied to the center of the receptive field. The conduction velocity of the individual bronchopulmonary afferent was calculated by dividing the distance along the nerve pathway by the time delay between the shock artifact and the action potential evoked by electrical stimulation. Mechanical stimulation was determined using manual application of calibrated von Frey fibers to the center of the receptive field. C-fibers were also characterized for their expression of TRPA1 and TRP vanilloid 1 (TRPV1) channels by their response to the selective TRPA1 agonist allyl isothiocyanate (AITC, 300 μM), and to the selective TRPV1 agonist capsaicin (1 μM). Chemical stimuli were intratracheally applied as a 1 ml bolus over 10 s. A response to either mechanical or chemical stimuli was considered positive if the number of action potentials in any 1 s bin was twice the average background response. All excitatory chemical treatments were separated by at least 15 mins wash. Due to potential heterologous desensitization, capsaicin was only given at the end of each experiment. Only those bronchopulmonary fibers that had a positive response to both mechanical and chemical stimuli were included in the study. Due to a lack of TRPV1 channels in bronchopulmonary C-fibers from TRPV1-/- mice, 'nociceptive' status was assessed solely by conduction velocity and the response to TRPA1 agonists (Kollarik et al., 2003; Nassenstein et al., 2008).

Determination of hyperexcitability via changes in mechanical threshold: The threshold for mechanical pressure required to evoke action potential discharge was determined by progressively decreasing the weight of von Frey fiber applied to the lung receptive field until no response was evoked. The least force required to evoke mechanically-induced action potential firing was then repeated once more to confirm threshold reproducibility (Riccio et al., 1996). The

Molecular Pharmacology Fast Forward. Published on March 18, 2014 as DOI: 10.1124/mol.113.091272
This article has not been copyedited and formatted. The final version may differ from this version.

lungs were then treated with antimycin A (20 μM). Ten minutes later von Frey fibers were used to determine the mechanical threshold again following mitochondrial modulation. Hyperexcitability was quantified by comparing the mechanical threshold before and after mitochondrial modulation (paired analysis). Due to the irreversible inhibition of complex III by antimycin (Stowe and Camara, 2009; Turrens et al., 1985), only one antimycin A treatment was used per preparation.

Determination of hyperexcitability via changes in response to chemical stimulus: We determined the action potential discharge response to α,β methylene ATP (α,β mATP, $P2X_{2/3}$ agonist, 30 μM) intratracheally applied as a 1 ml bolus over 10 s (Nassenstein et al., 2010). This submaximal dose is sufficient to activate all $P2X_{2/3}$ expressing bronchopulmonary C-fibers (Nassenstein et al., 2010). The lungs were then treated with antimycin A (20 μM) or other mitochondrial modulators. Ten minutes later the action potential discharge response to α,β mATP (30 μM) was again determined. Hyperexcitability to α,β mATP treatment was quantified in raw form in two ways: either by comparing the total number of action potentials discharged within 120s or comparing the peak response (maximum number of action potentials that occurred within any 1s bin) before and after mitochondrial modulation (both paired analyses). Due to variations in responsiveness to α,β mATP between bronchopulmonary C-fibers we also normalized each fiber's 2^{nd} response to α,β mATP to its 1^{st} α,β mATP response: (total number of action potentials discharged in 2^{nd} response / total number of action potentials discharged in 1^{st} response) X 100. This normalized quantification of excitability could then be compared between different treatment groups in our mechanistic studies (unpaired analysis). Due to the irreversible inhibition of complex III by antimycin (Stowe and Camara, 2009; Turrens et al., 1985), only one antimycin A treatment was used per preparation.

Molecular Pharmacology Fast Forward. Published on March 18, 2014 as DOI: 10.1124/mol.113.091272
This article has not been copyedited and formatted. The final version may differ from this version.

Knockout mice: Male TRPV1^{-}/$^{-}$ (Jackson Laboratory: B6.129X1-Trpv1tm1Jul/J) were mated with female TRPV1^{-}/$^{-}$. Genotype of offspring was confirmed by PCR.

Dissociation of mouse vagal ganglia: Male C57BL/6J mice were killed by CO_2 asphyxiation followed by exsanguination. Vagal ganglia were immediately isolated and enzymatically dissociated using previously described methods (Nesuashvili et al., 2013). Isolated neurons were plated onto poly-D-lysine and laminin-coated coverslips, incubated at 37°C in L-15 (supplemented with 10% FBS) and used within 24 hours.

PKC translocation immunocytochemistry: Dissociated mouse vagal neurons on glass coverslips were treated with either antimycin A (10 μM), phorbol-12-myristate-13-acetate (PMA, 300nM) or H_2O_2 (300 μM) by direct addition to culture media. Neurons were then fixed 2 minutes later using fresh 4% paraformaldehyde in order to preserve PKC subcellular location. In some cases antioxidants were applied to media prior to antimycin A: 90 minutes prior for tempol (1 mM); 15 minutes prior for MnTMPyP (50 μM). Neurons were then permeabilized using PBS containing 0.1% Triton X-100, for 10 min at room temperature and blocked using PBS with 0.0025% Tween-20 (PBST) containing 2% BSA for 45 min at room temperature. Cells were stained using a pan-PKC primary antibody (H-300; Santa-Cruz). Antibody concentrated to 0.5 mg/ml was diluted 1:50 in blocking buffer and left on cells overnight at 4^{o}C. Cells were washed 3 times using PBST then incubated with a CY5-labeled anti-rabbit secondary antibody (Life technologies, CA) diluted 1:1000 in blocking buffer and left on cells for 1 hr at room temperature. After 3 washes with PBST coverslips were mounted onto glass slides using VECTASHIELD(R) HardSet Mounting Medium with DAPI (Vector laboratories, CA). Imaging was performed using a Leica SP2 confocal microscope with a 63X objective: DAPI excitation of 405 nm, emission range of 415-480 nm; Cy5 excitation of 633 nm, emission range of 625-735

Molecular Pharmacology Fast Forward. Published on March 18, 2014 as DOI: 10.1124/mol.113.091272
This article has not been copyedited and formatted. The final version may differ from this version.

nm. Analysis of staining intensity was performed using ImageJ. A straight line was drawn across each cell in a region excluding the nucleus and the "Multi-plot" function was used to plot the profile of the staining. The ratio of the peak staining at the edge of the cell to the average staining across the center of the cell was generated to give the membrane/cytosolic ratio.

Statistical analysis: Data was analyzed using GraphPad software. Where appropriate paired or unpaired Student's T-test were used. A p value less than 0.05 was taken as significant. All data expressed as mean ± SEM.

Molecular Pharmacology Fast Forward. Published on March 18, 2014 as DOI: 10.1124/mol.113.091272
This article has not been copyedited and formatted. The final version may differ from this version.

RESULTS

Antimycin A decreases mechanical thresholds in nociceptive C-fibers

To study the effect of mitochondrial modulation on the excitability of bronchopulmonary C-fiber terminals, we have used a mouse ex vivo lung-vagal ganglia preparation. In this preparation the action potential discharge evoked in individual nerves by either mechanical or chemical stimuli to the airways can be quantified. Previous studies have shown that the majority of fibers innervating the lung are slowly conducting and express TRPA1 and TRPV1 (Nassenstein et al., 2008; Nesuashvili et al., 2013). This subset of nerves is thought to serve as nociceptors in the mouse airways. Here, we characterized bronchopulmonary sensory fibers based on their conduction velocity and their responsiveness to the selective TRPA1 and TRPV1 agonists (AITC and capsaicin, respectively). Bronchopulmonary fibers were considered nociceptive if they expressed TRPV1. As described before (Kollarik et al., 2003), TRPV1 expression was largely confined to fibers with conduction velocities <0.7m/s.

We first studied the effect of antimycin-induced mitochondrial modulation on the mechanical threshold for bronchopulmonary fibers using punctate stimuli of the lung tissue with von Frey fibers. All bronchopulmonary fibers are directly activated by punctate force (Kollarik et al., 2003; Nassenstein et al., 2008) in a P2X-independent manner (Weigand et al., 2012), and in this study a maximum von Frey stimulus (1.4g) evoked peak action discharge of 16.8 ± 1.7 Hz. Here, we determined the minimum force required to evoke action potential discharge in each fiber using the rationale that an increase in excitability would decrease the threshold for mechanically-induced action potential discharge (Riccio et al., 1996). Each fiber's threshold was stable over the duration of experimentation (Fig 1A). Antimycin A (20 μM) evoked significant action potential

Molecular Pharmacology Fast Forward. Published on March 18, 2014 as DOI: 10.1124/mol.113.091272
This article has not been copyedited and formatted. The final version may differ from this version.

discharge in TRPA1-expressing bronchopulmonary fibers via a ROS-dependent TRPA1 activation – this mechanism is described in our previous study (Nesuashvili et al., 2013). The direct activation of these TRPA1-expressing nerves lasted from 2-7 minutes, other fibers were not overtly activated. We tested the mechanical threshold 10 minutes following antimycin A treatment and compared with the mechanical threshold previous to antimycin A treatment. Antimycin A (20 μM) decreased the threshold for mechanical stimulation by approximately 50% in nociceptive neurons ($p<0.005$, n=13, Figs 1B, 1C). Seven of these 13 fibers were TRPA1-expressing nociceptors, but there was no correlation of expression of TRPA1 and the antimycin A-induced threshold decrement (not shown). However, antimycin A had no effect on the threshold for mechanical stimulation for faster conducting, non-nociceptive bronchopulmonary fibers ($p>0.05$, n=6, Fig 1C), which do not express TRPA1 or TRPV1.

Antimycin A increases excitability to chemical stimuli in nociceptive C-fibers

The standardization of manually-operated von Frey fiber mechanical stimulation of C-fibers can be challenging, particularly in a 3-dimensional tissue such as the lung. We therefore extended our study of mitochondrial modulation-induced hyperexcitability to determine its effects on bronchopulmonary C-fiber responses to chemical stimuli. Previous studies showed that the vast majority of mouse bronchopulmonary sensory nerves are activated by the selective $P2X_{2/3}$ agonist α,β mATP and that this response is reproducible (Kollarik et al., 2003; Nassenstein et al., 2010). Consistent with these reports, 30 μM α,β mATP activated >90% of bronchopulmonary C-fibers regardless of their conduction velocity or TRP channel expression. To confirm the reproducibility of $P2X_{2/3}$ receptor responses, we determined the action potential discharge to repeated treatment of 30 μM α,β mATP in 18 nociceptive C-fibers (separated by 15 minutes). There was no significant difference in either the total number of action potentials

Molecular Pharmacology Fast Forward. Published on March 18, 2014 as DOI: 10.1124/mol.113.091272
This article has not been copyedited and formatted. The final version may differ from this version.

evoked (1^{st}: 64.2 ± 9.5; 2^{nd}: 62.7 ± 11.1; Fig 2B) or the peak response (1^{st}: 17.7 ± 2.3 Hz; 2^{nd}: 15.9 ± 2.21 Hz; Fig 2C).

Ten minutes after treatment with 20 μM antimycin A, the response to 30 μM α,β mATP was significantly increased in nociceptive C-fibers (n=24, Fig 2A) as assessed by the total number of action potentials evoked (1^{st}: 105 ± 34.9; 2^{nd}: 220 ± 79.4; $p<0.01$) (Fig 2B), and the peak response (1^{st}: 15.4 ± 1.5 Hz; 2^{nd}: 20.5 ± 1.7 Hz; $p<0.01$) (Fig 2C). Similar to our mechanical threshold data, antimycin A failed to induce hyperexcitability to α,β mATP in non-nociceptive bronchopulmonary fibers (n=9).

The action potential discharge to α,β mATP varied significantly from nerve to nerve: out of 189 fibers examined in the present study the total number of action potentials evoked ranged from 16 to 280, and the peak discharge ranged from 3 to 37. To account for the intrinsic variability in neuronal responses, we quantified excitability by the change in the response to the 2^{nd} α,β mATP treatment (i.e. after antimycin A) as a percentage of each individual fiber's response to the 1^{st} α,β mATP treatment. As such, antimycin increased nociceptor excitability to 276 ± 54 % (n=24) compared to vehicle, which had no effect on excitability (105 ± 14 %, n=18, $p<0.005$)(see Figs 3B, 4A and 4B).

Given that our previous findings had shown that mitochondrial ROS evoked action potential discharge in nociceptors in a TRPA1-dependent manner, we compared the antimycin A-induced excitability in nociceptors that specifically expressed TRPA1 (n=8) with those nociceptors that did not express TRPA1 (n=16). Antimycin A increased excitability in both subsets of nociceptive C-fibers (Fig 3A), indicating that TRPA1 expression was not required for mitochondrial modulation-associated hyperexcitability to α,β mATP. There was a trend towards a greater

Molecular Pharmacology Fast Forward. Published on March 18, 2014 as DOI: 10.1124/mol.113.091272
This article has not been copyedited and formatted. The final version may differ from this version.

increase in excitability to α,β mATP in TRPA1-negative C-fibers – perhaps due to mild non-specific tachyphylaxis occurring following substantial TRPA1-mediated depolarization – although this did not reach statistical significance (p=0.19).

Our data demonstrating antimycin A evoked hyperexcitability only in nociceptors also led us to test the hypothesis that TRPV1, which is expressed exclusively in almost all nociceptors, was involved. Using a pretreatment of the selective TRPV1 antagonist iodoresiniferatoxin (1 μM, n=8) (Wahl et al., 2001), we found that antimycin A-induced sensitization to α,β mATP in nociceptors was not reduced (Fig 3B). In addition, we complemented these studies using ex vivo lung-vagal tissue from TRPV1-/- mice. Here, genetic ablation of TRPV1 failed to reduce antimycin A-induced nociceptor hyperexcitability to α,β mATP (n=14). We therefore conclude that despite the exclusivity of hyperexcitability in the nociceptive population, TRPV1 is not required for antimycin A-induced hyperexcitability to α,β mATP.

Comparisons with other mitochondrial modulators

The biochemical response to antimycin A is well characterized in isolated mitochondria and numerous cell types. Antimycin A selectively inhibits the Q_i site on complex III in the electron transport chain in the mitochondria, resulting in superoxide formation and the subsequent production of numerous ROS, mitochondrial membrane depolarization and a decrease in ATP production (Gyulkhandanyan and Pennefather, 2004; Stowe and Camara, 2009; Tretter et al., 2007; Turrens et al., 1985). Other specific complex inhibitors have also been described, in particular oligomycin and myxothiazol. Oligomycin inhibits complex V (also known as ATP synthase) and thus prevents ATP production by the oxidative phosphorylation machinery (Hool and Corry, 2007; Sipos et al., 2003). Inhibition of complex V also evokes a mild

Molecular Pharmacology Fast Forward. Published on March 18, 2014 as DOI: 10.1124/mol.113.091272
This article has not been copyedited and formatted. The final version may differ from this version.

hyperpolarization of the mitochondrial membrane potential but has little effect on superoxide production in most systems. Ten minutes following oligomycin (10 μM) treatment, there was no significant change in action potential discharge in response to α,β mATP (n=8, Fig 4A). Myxothiazol is a selective inhibitor of the Q_o site on complex III. Inhibition of Q_o causes mitochondrial membrane potential depolarization and a decrease in ATP production, but only evokes very mild superoxide production (Gyulkhandanyan and Pennefather, 2004; Tretter et al., 2007; Turrens et al., 1985). Ten minutes following myxothiazol (500nM) treatment, there was also no change in action potential discharge to α,β mATP (n=7, Fig 4A). These data suggest that antimycin A-induced nociceptor hyperexcitability to α,β mATP is not specifically due to a decrease in ATP production.

Involvement of ROS and PKC in antimycin A-induced hyperexcitability to α,β mATP

We hypothesized that antimycin A-induced nociceptor hyperexcitability to α,β mATP was mediated by the actions of mitochondrially-derived ROS. Many biological actions of ROS are due to their ability to oxidize protein residues (e.g. cysteine), which can be reversed by a reducing agent such as dithiothreitol (DTT) or by quenching with a cysteine antioxidant such as N-acetyl-cysteine (NAC) or glutathione (GSH). DTT is membrane permeable. NAC is slowly actively transported across plasma membranes (Raftos et al., 2007) and has previously been shown to quench intracellular ROS pathways (Hongpaisan et al., 2004; Takahashi et al., 2011). GSH is membrane impermeable and is not subject to active transport as NAC is (Raftos et al., 2007). We tested the contribution of oxidation to antimycin A-induced hyperexcitability by treating the lungs with DTT (1mM) or NAC (1mm) or GSH (1mM) for 10 minutes prior to and during antimycin A (20 μM) treatment. Both DTT (n=4) and NAC (n=8) completely abolished the antimycin A-induced increase in excitability to α,β mATP ($p<0.01$ compared to antimycin A

Molecular Pharmacology Fast Forward. Published on March 18, 2014 as DOI: 10.1124/mol.113.091272
This article has not been copyedited and formatted. The final version may differ from this version.

alone), whereas GSH (n=4) failed to inhibit the antimycin A-induced hyperexcitability to α,β mATP ($p<0.005$ compared to vehicle (no antimycin), $p=0.17$ compared to antimycin A alone) (Fig 4B). Based on the differential distribution of GSH (extracellular) and NAC (extracellular and intracellular), this data suggests that intraneuronal ROS contribute to the antimycin A-induced hyperexcitability to α,β mATP.

Selective inhibition of Q_o using myxothiazol is known to substantially reduce subsequent superoxide production evoked by inhibition of the Q_i site (antimycin A) (Gyulkhandanyan and Pennefather, 2004; Tretter et al., 2007; Turrens et al., 1985). We have previously shown that myxothiazol pretreatment prior to antimycin A greatly reduced antimycin A-induced TRPA1 activation (Nesuashvili et al., 2013). Here, we pretreated the lungs with myxothiazol (500nM) three minutes prior to antimycin A (20 μM) treatment. Myxothiazol prevented the development of antimycin A-induced nociceptor hyperexcitability to α,β mATP (Fig 4B): for antimycin alone the response to the 2nd α,β mATP was 276 ± 54 % (n=24); with myxothiazol pretreatment of antimycin A the response to the 2nd α,β mATP was 128 ± 41 % (n=9, $p<0.05$). These findings suggest that ROS evoked from mitochondrial complex III are required for antimycin A-induced hyperexcitability to α,β mATP.

Numerous studies of dorsal root ganglion (DRG) nociceptors involved in somatosensory pain have shown that protein kinase C (PKC) is a powerful regulator of nociceptor excitability (Baker, 2005; Cesare et al., 1999; Wu et al., 2012). Interestingly, there has been increasing evidence that many PKC isoforms can be activated by cellular oxidants (e.g. superoxide and H_2O_2) independently of either Ca^{2+} or lipid mediators such as DAG (Cosentino-Gomes et al., 2012; Gopalakrishna and Anderson, 1989; Knapp and Klann, 2000). We hypothesized that mitochondrial ROS induces airway nociceptor hyperexcitability to α,β mATP via activation of

Molecular Pharmacology Fast Forward. Published on March 18, 2014 as DOI: 10.1124/mol.113.091272
This article has not been copyedited and formatted. The final version may differ from this version.

protein kinase C. For these studies we used a selective PKC inhibitor called bisindolylmaleimide I (BIM I, also known as GF 109203X and Gö 6850) and its inactive analog BIM V (also known as Ro 31-6045). These compounds are membrane permeable and differ in only one side chain. BIM I is a potent PKC inhibitor with an IC_{50} below 500nM, whereas BIM V has an IC_{50} for PKC >100 μM (Davis et al., 1992; Toullec et al., 1991). When the lungs were pretreated with BIM I (1 μM) for ten minutes prior to and during antimycin A (20 μM) treatment there was no increase in nociceptor hyperexcitability: the response to the 2nd α,β mATP was only 136 ± 16 % (n=14, p<0.01 compared to antimycin A alone)(Fig 4B). However, pretreatment with the inactive analog BIM V (1 μM) for ten minutes prior to and during antimycin A (20 μM) treatment failed to prevent antimycin A-induced nociceptor hyperexcitability: the response to the 2nd α,β mATP was 231 ± 56 % (n=20, p<0.05 compared to vehicle (no antimycin), p=0.28 compared to antimycin A alone)(Fig 4B). These data suggest that antimycin A-induced nociceptor hyperexcitability to α,β mATP is dependent on the actions of PKC.

Lastly we determined whether or not PKC activation or ROS were sufficient to evoke vagal bronchopulmonary C-fiber hyperexcitability in the absence of mitochondrial dysfunction by antimycin A. PMA is a potent and selective activator of PKC. As before in the antimycin A studies the nociceptor action potential response to 30 μM α,β mATP was determined. Then the lungs were treated with 3 μM PMA and the response to α,β mATP was determined two minutes later. As expected, PMA induced nociceptor hyperexcitability to α,β mATP: the response to the 2nd α,β mATP was 267 ± 111 % (n=11, p<0.05 compared to vehicle)(Fig 5). Using a similar protocol we found that exogenously applied H_2O_2 also induced airway nociceptor hyperexcitability to α,β mATP: two minutes after H_2O_2 (1mM) the response to the 2nd α,β mATP was 207 ± 35 % (n=15, p<0.01 compared to vehicle)(Fig 5). Consistent with the mechanism of antimycin A-induced hyperexcitability to α,β mATP, H_2O_2-induced hyperexcitability to α,β mATP

Molecular Pharmacology Fast Forward. Published on March 18, 2014 as DOI: 10.1124/mol.113.091272
This article has not been copyedited and formatted. The final version may differ from this version.

was prevented by pretreatment with the selective PKC inhibitor BIM I (1 μM): the response to the 2nd α,β mATP was only 89 ± 8 % (n=5, p<0.005 compared to H2O2 alone)(Fig 5).

Some of the airway C-fibers (8 out of 16) used in the H_2O_2 hyperexcitability studies expressed TRPA1 (as determined by sensitivity to AITC). Although not the focus of this study, TRPA1 has been shown to be activated by H_2O_2 in vitro (Andersson et al., 2008). Consistent with those findings, H_2O_2 robustly activated TRPA1-expressing C-fibers (peak discharge of 6.4 ± 1.8 Hz) compared to those C-fibers that did not express TRPA1 (peak discharge of 0.6 ± 0.6 Hz). H_2O_2-induced C-fiber activation was short-lived and the response was absent prior to the 2nd α,β mATP stimulus. As with antimycin A-induced hyperexcitability to α,β mATP, the H_2O_2-induced hyperexcitability to α,β mATP was unaffected by the presence or absence of TRPA1 (data not shown).

Antimycin A induces PKC translocation in vagal neurons

Critical to PKC activity is its subcellular location (Cosentino-Gomes et al., 2012). Typically PKC isoforms remain in the cytosol while inactive. Upon activation, PKC translocates to the plasma membrane where it engages in phosphorylation of a wide variety of protein targets. Given that previous studies demonstrated multiple isoforms of PKC heterogeneously expressed throughout the somatosensory DRG neuronal population (Cesare et al., 1999; Hayase et al., 2007; Wu et al., 2012; Zhang et al., 2012) and that PKC isoform expression has not yet been characterized in vagal neurons we decided here to observe global PKC translocation using a pan-PKC antibody that would detect all PKC isoforms. All vagal neurons were immunoreactive for PKC with no fluorescent signal observed in the absence of primary antibody (not shown). In control conditions, the vast majority of PKC immunoreactivity was located in the cytosol (n=225)(Fig 6).

Molecular Pharmacology Fast Forward. Published on March 18, 2014 as DOI: 10.1124/mol.113.091272
This article has not been copyedited and formatted. The final version may differ from this version.

As expected there was a significant increase in PKC immunoreactivity at the plasma membrane two minutes after PMA (300nM) treatment (n=216, $p<0.0001$ compared to control), indicating that activation of PKC causes translocation to the plasma membrane. Consistent with our electrophysiological data at the airway vagal nerve terminal, antimycin A (10 μM) induced significant PKC translocation to the plasma membrane (n=134, $p<0.0005$ compared to control). Antimycin A-induced PKC translocation was abolished by the pretreatment of the neurons with a combination of the antioxidants tempol (1mM) and MnTMPyP (50 μM)(n=41, $p<0.05$ compared to antimycin alone), indicating a critical role of mitochondrial ROS in these responses. Finally, we found that exogenously applied H_2O_2 (300 μM) was sufficient to induce significant PKC translocation to the membrane (n=173, $p<0.005$ compared to control). Overall, these data indicate that mitochondrial ROS induce PKC translocation, consistent with a role of PKC in mitochondrial ROS-induced airway nociceptor hyperexcitability.

Molecular Pharmacology Fast Forward. Published on March 18, 2014 as DOI: 10.1124/mol.113.091272
This article has not been copyedited and formatted. The final version may differ from this version.

DISCUSSION

Inflammation alters mitochondrial function (Sena and Chandel, 2012). Given that peripheral sensory nerve terminals are densely packed with mitochondria (Hung et al., 1973; von During and Andres, 1988), we investigated the effect of mitochondrial modulation on sensory nerve terminal excitability. In this study ROS evoked by mitochondrial dysfunction induced hyperexcitability to both mechanical and chemical stimuli in nociceptive bronchopulmonary C-fibers but had little effect on the excitability of non-nociceptive nerves. Nociceptive nerves protect the innervated organ through the initiation of reflexes and behavioral responses (Carr and Undem, 2003), and hyperexcitability contributes to aberrant signs and symptoms in inflammatory and infectious states (Carr and Lee, 2005; Meyer et al., 1996). Thus we present evidence of a novel mechanism by which nocifensive airway responses can be inappropriately modulated.

There are two subtypes of mouse vagal bronchopulmonary C-fibers: slowly-conducting C-fibers express various “nociceptor” receptors such as TRPV1 (Kollarik et al., 2003) and are thought to be synonymous with nociceptive afferents in humans that mediate cough, dyspnea and reflex bronchospasm (Carr and Undem, 2003); faster-conducting C-fibers do not express TRPV1 and are considered to be non-nociceptive – perhaps involved in regulation of eupnic breathing. We previously demonstrated that antimycin A, a Q_i site inhibitor of the electron transfer chain complex III that induces production of mitochondrial ROS (Stowe and Camara, 2009), caused the activation of nociceptive C-fibers via the activation of another “nociceptive” ion channel TRPA1 (Nesuashvili et al., 2013). This activation typically lasted 2-7 minutes. Here, we found that antimycin A evoked a profound increase in nociceptive C-fiber excitability as determined by decreased threshold for punctate mechanical stimulation and by increased action potential

Molecular Pharmacology Fast Forward. Published on March 18, 2014 as DOI: 10.1124/mol.113.091272
This article has not been copyedited and formatted. The final version may differ from this version.

discharge to α,β mATP, an agonist for $P2X_{2/3}$ ion channels. Antimycin A failed to increase non-nociceptive nerve excitability. Unlike antimycin A-induced C-fiber activation (Nesuashvili et al., 2013), antimycin A-induced hyperexcitability to α,β mATP was not dependent on the expression of TRPA1. Despite the exclusivity of hyperexcitability in the TRPV1-expressing nociceptive population, TRPV1 was also not required for antimycin A-induced hyperexcitability to α,β mATP. We briefly investigated the effect of 1mM H_2O_2 on nociceptor activation and found that activation correlated with sensitivity to the TRPA1 agonist AITC. This is consistent with other studies using similar doses (Andersson et al., 2008), although studies using 120mM H_2O_2 suggest that, along with TRPA1, P2X channels also contribute to H_2O_2-induced C-fiber activation (Lin et al., 2013).

Our mechanistic studies suggest that antimycin A evokes airway nociceptor hyperexcitability to α,β mATP via the actions of ROS and PKC, largely independent of mitochondrial ATP production. Antimycin A, oligomycin (complex V inhibitor) and myxothiazol (complex III Q_o site inhibitor) all decrease ATP production, but only antimycin A causes significant mitochondrial superoxide production (Stowe and Camara, 2009) and only antimycin A evoked significant nociceptor hyperexcitability in this study. Furthermore, myxothiazol, which prevents antimycin A-induced ROS production, prevented antimycin A-induced hyperexcitability, indicating that the hyperexcitability was specifically due to ROS produced from the complex III Q_o site. It should be noted that we have not measured ROS or ATP production from the nerve terminals in this study. The potency of oligomycin, antimycin A and myxothiazol used in their single concentrations on ROS or ATP production cannot be confirmed and thus caution must be employed in drawing conclusions. Nevertheless, the concentrations were chosen from previous studies showing the selective effects of inhibition of ATP synthase (oligomycin), complex III Q_i site (antimycin A) and complex III Q_o site (myxothiazol) on ROS production, ATP production and oxygen consumption (Gyulkhandanyan and Pennefather, 2004; Hool and Corry, 2007; Sipos et al., 2003; Stowe and

Molecular Pharmacology Fast Forward. Published on March 18, 2014 as DOI: 10.1124/mol.113.091272
This article has not been copyedited and formatted. The final version may differ from this version.

Camara, 2009; Tretter et al., 2007; Turrens et al., 1985). The role of ROS in this pathway was confirmed by the inhibition of antimycin A-induced hyperexcitability by the antioxidant NAC (detoxifies ROS) and the reducing agent DTT (reverses sulfhydryl group oxidation). NAC is actively transported across the plasma membrane unlike the antioxidant GSH (Raftos et al., 2007). GSH (only detoxifies extracellular ROS) failed to inhibit antimycin A-induced hyperexcitability, indicating that intracellular (i.e. intraneuronal) ROS contributed significantly to this phenomenon. It is not known if superoxide or other downstream ROS (e.g. H_2O_2) are the end effectors of mitochondrial modulation-induced hyperexcitability, but the inhibition by DTT would argue against a significant role of lipid peroxidation products, which react with proteins in a DTT-insensitive manner (Andersson et al., 2008).

Antimycin A and H_2O_2 caused nociceptor hyperexcitability to α,β mATP that was sensitive to the selective PKC inhibitor BIM I but not to its inactive analogue BIM V. Selectivity is a relative term for kinase inhibitors, but at 1 μM BIM I inhibits PKC without affecting protein kinase A; and the other off-target effects of bisindolylmaleimide compounds are shared by both BIM I and BIM V (Davis et al., 1992; Toullec et al., 1991). That PKC activation could lead to nociceptor hyperexcitability was further demonstrated by PMA, an activator of PKC, which produced hyperexcitability of a similar magnitude to antimycin A and H_2O_2. PMA and the activation of PKC has been shown previously to induce hyperexcitability in vagal nociceptive neurons (Gu and Lee, 2006; Gu and Lee, 2009; Ikeda et al., 2005; Kagaya et al., 2002; Matsumoto et al., 2007). PKC translocation from the cytosol to the plasma membrane is an indicator of PKC activation (Cosentino-Gomes et al., 2012). Our electrophysiological studies were supported by confocal imaging in dissociated neurons indicating that antimycin A and H_2O_2 both induced PKC translocation. Antimycin A-induced PKC translocation was prevented by a combination of

Molecular Pharmacology Fast Forward. Published on March 18, 2014 as DOI: 10.1124/mol.113.091272
This article has not been copyedited and formatted. The final version may differ from this version.

tempol (superoxide dismutase mimetic) and MnTMPyP (combined superoxide dismutase and catalase mimetic), indicating that ROS were required for this effect.

There are fifteen PKC isoforms, which are divided into three groups based upon sensitivity to Ca^{2+} and DAG: classical isoforms (α, β and γ) require both Ca^{2+} and DAG for activation, novel isoforms (δ, ε, η and θ) require DAG but not Ca^{2+} for activation and atypical isoforms (ι/λ and ζ) require neither Ca^{2+} nor DAG for activation. To date there has not been any characterization of PKC isoform expression in vagal sensory neurons, although PKC expression in somatosensory DRG neurons indicates that at a minimum β1, β2, δ, ε and ζ are expressed in complex combinatorial patterns (Cesare et al., 1999; Wu et al., 2012). Similar to our findings PKC has repeatedly been shown to play a role in inflammation-induced hyperexcitability in nociceptive DRG (Baker, 2005; Cesare et al., 1999; Wu et al., 2012; Zhang et al., 2012). It is known that PMA binds to the same enzyme subsite as DAG and thus PMA activates only classical and novel PKC isoforms, suggesting that PKC expression is not limited to atypical isoforms in vagal sensory nerves. Although ROS activate PKC by the oxidation of cysteines in a pair of zinc fingers associated with the DAG binding site (Gopalakrishna and Anderson, 1989; Knapp and Klann, 2000), this does not preclude the contribution of atypical isoforms that are activated by the same mechanism on their single zinc finger site (that does not bind DAG) (Cosentino-Gomes et al., 2012). Further studies are required to elucidate which PKC isoform is involved in mitochondrial ROS-induced bronchopulmonary C-fiber hyperexcitability.

Another question raised by these studies is how does activation of PKC cause hyperexcitability in vagal bronchopulmonary C-fibers? Activated PKC isoforms are capable of modifying neuronal excitability via the phosphorylation of numerous cellular targets including ion channels and transporters. In particular, PKC has been shown to induce hyperexcitability via tetrodotoxin-

Molecular Pharmacology Fast Forward. Published on March 18, 2014 as DOI: 10.1124/mol.113.091272
This article has not been copyedited and formatted. The final version may differ from this version.

resistant voltage-gated Na+ channels in both vagal (Ikeda et al., 2005; Kagaya et al., 2002; Matsumoto et al., 2007) and DRG neurons (Baker, 2005; Hayase et al., 2007; Wu et al., 2012), indicating possible candidates for mitochondrial ROS-induced bronchopulmonary C-fiber hyperexcitability. However, given that tetrodotoxin-resistant voltage-gated Na+ channels are expressed in both nociceptive and non-nociceptive neurons (Kwong et al., 2008), further work is needed to elucidate the mechanism highlighted in the present study and its apparent exclusivity to nociceptive C-fibers.

In summary, we have found that antimycin A causes a robust increase in bronchopulmonary C-fiber excitability via the actions of mitochondrial ROS and PKC. Mitochondrial ROS are known to increase excitability in CNS neurons (Nozoe et al., 2008; Yin et al., 2010), to activate vagal nociceptive neurons (Nesuashvili et al., 2013) and to regulate Ca^{2+} signaling in DRG nociceptive neurons (Kim and Usachev, 2009). Airway inflammatory disease is associated with mitochondrial dysfunction and mitochondrial ROS production (Aguilera-Aguirre et al., 2009; Mabalirajan et al., 2008; Reddy, 2011) and a wide variety of inflammatory signaling has been shown to increase mitochondrial ROS (Bell et al., 2007; Corda et al., 2001; Michaeloudes et al., 2010; Pehar et al., 2007; West et al., 2011). Given the mitochondrial density within sensory nerve terminals it is possible that inflammation may induce nociceptor hyperexcitability via the production of mitochondrial ROS. It is now increasingly clear that, in addition to initiating apoptosis, mitochondrial dysfunction and ROS production also contribute to more subtle physiological signaling (Sena and Chandel, 2012), and it remains to be determined if chronic mitochondrial ROS in sensory nerve terminals contribute to hyperreflexia in airway disease.

Molecular Pharmacology Fast Forward. Published on March 18, 2014 as DOI: 10.1124/mol.113.091272
This article has not been copyedited and formatted. The final version may differ from this version.

AUTHOR CONTRIBUTIONS:

Participated in research design: Bahia, Taylor-Clark

Conducted experiments: Hadley, Bahia

Performed data analysis: Hadley, Bahia, Taylor-Clark

Contributed to the writing of the manuscript: Bahia, Taylor-Clark

Molecular Pharmacology Fast Forward. Published on March 18, 2014 as DOI: 10.1124/mol.113.091272
This article has not been copyedited and formatted. The final version may differ from this version.

REFERENCES

Aguilera-Aguirre L, Bacsi A, Saavedra-Molina A, Kurosky A, Sur S and Boldogh I (2009) Mitochondrial dysfunction increases allergic airway inflammation. *J Immunol* **183**(8): 5379-5387.

Amadesi S, Nie J, Vergnolle N, Cottrell GS, Grady EF, Trevisani M, Manni C, Geppetti P, McRoberts JA, Ennes H, Davis JB, Mayer EA and Bunnett NW (2004) Protease-activated receptor 2 sensitizes the capsaicin receptor transient receptor potential vanilloid receptor 1 to induce hyperalgesia. *J Neurosci* **24**(18): 4300-4312.

Andersson DA, Gentry C, Moss S and Bevan S (2008) Transient receptor potential A1 is a sensory receptor for multiple products of oxidative stress. *J Neurosci* **28**(10): 2485-2494.

Baker MD (2005) Protein kinase C mediates up-regulation of tetrodotoxin-resistant, persistent Na+ current in rat and mouse sensory neurones. *J Physiol* **567**(Pt 3): 851-867.

Bell EL, Klimova TA, Eisenbart J, Moraes CT, Murphy MP, Budinger GR and Chandel NS (2007) The Qo site of the mitochondrial complex III is required for the transduction of hypoxic signaling via reactive oxygen species production. *J Cell Biol* **177**(6): 1029-1036.

Carr MJ and Lee LY (2005) Plasticity of peripheral mechanisms of cough. *Respir Physiol Neurobiol*.

Carr MJ and Undem BJ (2003) Bronchopulmonary afferent nerves. *Respirology* **8**(3): 291-301.

Cesare P, Dekker LV, Sardini A, Parker PJ and McNaughton PA (1999) Specific involvement of PKC-epsilon in sensitization of the neuronal response to painful heat. *Neuron* **23**(3): 617-624.

Corda S, Laplace C, Vicaut E and Duranteau J (2001) Rapid reactive oxygen species production by mitochondria in endothelial cells exposed to tumor necrosis factor-alpha is mediated by ceramide. *Am J Respir Cell Mol Biol* **24**(6): 762-768.

Molecular Pharmacology Fast Forward. Published on March 18, 2014 as DOI: 10.1124/mol.113.091272
This article has not been copyedited and formatted. The final version may differ from this version.

Cosentino-Gomes D, Rocco-Machado N and Meyer-Fernandes JR (2012) Cell Signaling through Protein Kinase C Oxidation and Activation. *Int J Mol Sci* **13**(9): 10697-10721.

Davis PD, Hill CH, Lawton G, Nixon JS, Wilkinson SE, Hurst SA, Keech E and Turner SE (1992) Inhibitors of protein kinase C. 1. 2,3-Bisarylmaleimides. *J Med Chem* **35**(1): 177-184.

Gopalakrishna R and Anderson WB (1989) Ca2+- and phospholipid-independent activation of protein kinase C by selective oxidative modification of the regulatory domain. *Proc Natl Acad Sci U S A* **86**(17): 6758-6762.

Gu Q and Lee LY (2006) Hypersensitivity of pulmonary chemosensitive neurons induced by activation of protease-activated receptor-2 in rats. *J Physiol* **574**(Pt 3): 867-876.

Gu Q and Lee LY (2009) Effect of protease-activated receptor 2 activation on single TRPV1 channel activities in rat vagal pulmonary sensory neurons. *Exp Physiol* **94**(8): 928-936.

Gyulkhandanyan AV and Pennefather PS (2004) Shift in the localization of sites of hydrogen peroxide production in brain mitochondria by mitochondrial stress. *J Neurochem* **90**(2): 405-421.

Hayase F, Matsuura H, Sanada M, Kitada-Hamada K, Omatsu-Kanbe M, Maeda K, Kashiwagi A and Yasuda H (2007) Inhibitory action of protein kinase Cbeta inhibitor on tetrodotoxin-resistant Na+ current in small dorsal root ganglion neurons in diabetic rats. *Neurosci Lett* **417**(1): 90-94.

Hongpaisan J, Winters CA and Andrews SB (2004) Strong calcium entry activates mitochondrial superoxide generation, upregulating kinase signaling in hippocampal neurons. *J Neurosci* **24**(48): 10878-10887.

Hool LC and Corry B (2007) Redox control of calcium channels: from mechanisms to therapeutic opportunities. *Antioxid Redox Signal* **9**(4): 409-435.

Hung KS, Hertweck MS, Hardy JD and Loosli CG (1973) Ultrastructure of nerves and associated cells in bronchiolar epithelium of the mouse lung. *J Ultrastruct Res* **43**(5): 426-437.

Molecular Pharmacology Fast Forward. Published on March 18, 2014 as DOI: 10.1124/mol.113.091272
This article has not been copyedited and formatted. The final version may differ from this version.

Ikeda M, Yoshida S, Kadoi J, Nakano Y and Mastumoto S (2005) The effect of PKC activity on the TTX-R sodium currents from rat nodose ganglion neurons. *Life Sci* **78**(1): 47-53.

Jesenak M, Babusikova E, Petrikova M, Turcan T, Rennerova Z, Michnova Z, Havlicekova Z, Villa MP and Banovcin P (2009) Cough reflex sensitivity in various phenotypes of childhood asthma. *J Physiol Pharmacol* **60 Suppl 5**: 61-65.

Kagaya M, Lamb J, Robbins J, Page CP and Spina D (2002) Characterization of the anandamide induced depolarization of guinea-pig isolated vagus nerve. *Br J Pharmacol* **137**(1): 39-48.

Kim MS and Usachev YM (2009) Mitochondrial Ca2+ cycling facilitates activation of the transcription factor NFAT in sensory neurons. *J Neurosci* **29**(39): 12101-12114.

Knapp LT and Klann E (2000) Superoxide-induced stimulation of protein kinase C via thiol modification and modulation of zinc content. *J Biol Chem* **275**(31): 24136-24145.

Kollarik M, Dinh QT, Fischer A and Undem BJ (2003) Capsaicin-sensitive and -insensitive vagal bronchopulmonary C-fibres in the mouse. *J Physiol* **551**(Pt 3): 869-879.

Kwong K, Carr MJ, Gibbard A, Savage TJ, Singh K, Jing J, Meeker S and Undem BJ (2008) Voltage-gated sodium channels in nociceptive versus non-nociceptive nodose vagal sensory neurons innervating guinea pig lungs. *J Physiol* **586**(5): 1321-1336.

Lin YJ, Hsu HH, Ruan T and Kou YR (2013) Mediator mechanisms involved in TRPV1, TRPA1 and P2X receptor-mediated sensory transduction of pulmonary ROS by vagal lung C-fibers in rats. *Respir Physiol Neurobiol* **189**(1): 1-9.

Mabalirajan U, Dinda AK, Kumar S, Roshan R, Gupta P, Sharma SK and Ghosh B (2008) Mitochondrial structural changes and dysfunction are associated with experimental allergic asthma. *J Immunol* **181**(5): 3540-3548.

Matsumoto S, Yoshida S, Ikeda M, Tanimoto T, Saiki C, Takeda M, Shima Y and Ohta H (2007) Effect of 8-bromo-cAMP on the tetrodotoxin-resistant sodium (Nav 1.8) current in small-diameter nodose ganglion neurons. *Neuropharmacology* **52**(3): 904-924.

Molecular Pharmacology Fast Forward. Published on March 18, 2014 as DOI: 10.1124/mol.113.091272
This article has not been copyedited and formatted. The final version may differ from this version.

Meyer RA, Raja SN and Cambell JN (1996) Neural mechanisms of primary hyperalgesia, in *Neurobiology of Nociceptors* (Belmonte C and Cervero F eds) pp 370-389, Oxford University Press.

Michaeloudes C, Sukkar MB, Khorasani NM, Bhavsar PK and Chung KF (2010) TGF-{beta} regulates Nox4, MnSOD and catalase expression and IL-6 release in airway smooth muscle cells. *Am J Physiol Lung Cell Mol Physiol*.

Morice AH (2010) The cough hypersensitivity syndrome: a novel paradigm for understanding cough. *Lung* **188 Suppl 1**: S87-90.

Nassenstein C, Kammertoens T, Veres TZ, Uckert W, Spies E, Fuchs B, Krug N and Braun A (2007) Neuroimmune crosstalk in asthma: dual role of the neurotrophin receptor p75NTR. *J Allergy Clin Immunol* **120**(5): 1089-1096.

Nassenstein C, Kwong K, Taylor-Clark T, Kollarik M, Macglashan DM, Braun A and Undem BJ (2008) Expression and function of the ion channel TRPA1 in vagal afferent nerves innervating mouse lungs. *J Physiol* **586**(6): 1595-1604.

Nassenstein C, Taylor-Clark TE, Myers AC, Ru F, Nandigama R, Bettner W and Undem BJ (2010) Phenotypic distinctions between neural crest and placodal derived vagal C-fibres in mouse lungs. *J Physiol* **588**(Pt 23): 4769-4783.

Nesuashvili L, Hadley SH, Bahia PK and Taylor-Clark TE (2013) Sensory nerve terminal mitochondrial dysfunction activates airway sensory nerves via transient receptor potential (TRP) channels. *Mol Pharmacol* **83**(5): 1007-1019.

Nozoe M, Hirooka Y, Koga Y, Araki S, Konno S, Kishi T, Ide T and Sunagawa K (2008) Mitochondria-derived reactive oxygen species mediate sympathoexcitation induced by angiotensin II in the rostral ventrolateral medulla. *J Hypertens* **26**(11): 2176-2184.

Pehar M, Vargas MR, Robinson KM, Cassina P, Diaz-Amarilla PJ, Hagen TM, Radi R, Barbeito L and Beckman JS (2007) Mitochondrial superoxide production and nuclear factor

erythroid 2-related factor 2 activation in p75 neurotrophin receptor-induced motor neuron apoptosis. *J Neurosci* **27**(29): 7777-7785.

Raftos JE, Whillier S, Chapman BE and Kuchel PW (2007) Kinetics of uptake and deacetylation of N-acetylcysteine by human erythrocytes. *Int J Biochem Cell Biol* **39**(9): 1698-1706.

Reddy PH (2011) Mitochondrial Dysfunction and Oxidative Stress in Asthma: Implications for Mitochondria-Targeted Antioxidant Therapeutics. *Pharmaceuticals (Basel)* **4**(3): 429-456.

Riccio MM, Myers AC and Undem BJ (1996) Immunomodulation of afferent neurons in guinea-pig isolated airway. *J Physiol* **491 (Pt 2)**: 499-509.

Sabogal C, Auais A, Napchan G, Mager E, Zhou BG, Suguihara C, Bancalari E and Piedimonte G (2005) Effect of respiratory syncytial virus on apnea in weanling rats. *Pediatr Res* **57**(6): 819-825.

Sena LA and Chandel NS (2012) Physiological roles of mitochondrial reactive oxygen species. *Mol Cell* **48**(2): 158-167.

Sipos I, Tretter L and Adam-Vizi V (2003) Quantitative relationship between inhibition of respiratory complexes and formation of reactive oxygen species in isolated nerve terminals. *J Neurochem* **84**(1): 112-118.

Stowe DF and Camara AK (2009) Mitochondrial reactive oxygen species production in excitable cells: modulators of mitochondrial and cell function. *Antioxid Redox Signal* **11**(6): 1373-1414.

Takahashi N, Kuwaki T, Kiyonaka S, Numata T, Kozai D, Mizuno Y, Yamamoto S, Naito S, Knevels E, Carmeliet P, Oga T, Kaneko S, Suga S, Nokami T, Yoshida J and Mori Y (2011) TRPA1 underlies a sensing mechanism for O2. *Nat Chem Biol* **7**(10): 701-711.

Thannickal VJ and Fanburg BL (2000) Reactive oxygen species in cell signaling. *Am J Physiol Lung Cell Mol Physiol* **279**(6): L1005-1028.

Toullec D, Pianetti P, Coste H, Bellevergue P, Grand-Perret T, Ajakane M, Baudet V, Boissin P, Boursier E, Loriolle F and et al. (1991) The bisindolylmaleimide GF 109203X is a potent and selective inhibitor of protein kinase C. *J Biol Chem* **266**(24): 15771-15781.

Tretter L, Takacs K, Hegedus V and Adam-Vizi V (2007) Characteristics of alpha-glycerophosphate-evoked H2O2 generation in brain mitochondria. *J Neurochem* **100**(3): 650-663.

Turrens JF, Alexandre A and Lehninger AL (1985) Ubisemiquinone is the electron donor for superoxide formation by complex III of heart mitochondria. *Arch Biochem Biophys* **237**(2): 408-414.

von During M and Andres KH (1988) Structure and functional anatomy of visceroreceptors in the mammalian respiratory system. *Prog Brain Res* **74**: 139-154.

Wahl P, Foged C, Tullin S and Thomsen C (2001) Iodo-resiniferatoxin, a new potent vanilloid receptor antagonist. *Mol Pharmacol* **59**(1): 9-15.

Weigand LA, Ford AP and Undem BJ (2012) A role for ATP in bronchoconstriction-induced activation of guinea pig vagal intrapulmonary C-fibres. *J Physiol* **590**(Pt 16): 4109-4120.

West AP, Brodsky IE, Rahner C, Woo DK, Erdjument-Bromage H, Tempst P, Walsh MC, Choi Y, Shadel GS and Ghosh S (2011) TLR signalling augments macrophage bactericidal activity through mitochondrial ROS. *Nature* **472**(7344): 476-480.

Wu DF, Chandra D, McMahon T, Wang D, Dadgar J, Kharazia VN, Liang YJ, Waxman SG, Dib-Hajj SD and Messing RO (2012) PKCepsilon phosphorylation of the sodium channel NaV1.8 increases channel function and produces mechanical hyperalgesia in mice. *J Clin Invest* **122**(4): 1306-1315.

Yin JX, Yang RF, Li S, Renshaw AO, Li YL, Schultz HD and Zimmerman MC (2010) Mitochondria-produced superoxide mediates angiotensin II-induced inhibition of neuronal potassium current. *Am J Physiol Cell Physiol* **298**(4): C857-865.

Molecular Pharmacology Fast Forward. Published on March 18, 2014 as DOI: 10.1124/mol.113.091272
This article has not been copyedited and formatted. The final version may differ from this version.

Zhang YH, Kays J, Hodgdon KE, Sacktor TC and Nicol GD (2012) Nerve growth factor enhances the excitability of rat sensory neurons through activation of the atypical protein kinase C isoform, PKMzeta. *J Neurophysiol* **107**(1): 315-335.

Molecular Pharmacology Fast Forward. Published on March 18, 2014 as DOI: 10.1124/mol.113.091272
This article has not been copyedited and formatted. The final version may differ from this version.

FOOTNOTES

This work has been supported by the NIH [R00HL088520 and R01HL119802].

Reprints requests: Thomas E Taylor-Clark, 12901 Bruce B Downs Blvd, Tampa, Florida 33612, USA. ttaylorc@health.usf.edu

Molecular Pharmacology Fast Forward. Published on March 18, 2014 as DOI: 10.1124/mol.113.091272
This article has not been copyedited and formatted. The final version may differ from this version.

LEGENDS

Fig 1. **Antimycin A decreases the threshold required for mechanical stimulation in nociceptive C-fibers.** A, representative trace of action potential discharge elicited by von Frey fibers (a = 0.4g (threshold), b = 0.16g (sub-threshold)) in a nociceptive bronchopulmonary C-fiber (defined by conduction velocity (CV) and sensitivity to capsaicin (not shown)). Inserts show magnified timescale of responses. B, representative trace of mechanical threshold determination in a nociceptive bronchopulmonary C-fiber before (control) and 10 minutes after treatment with antimycin A (20 μM). Application of von Frey stimulus denoted by arrows. C, mean ± SEM mechanical threshold for action potential discharge before (control, hatched bars) and 10 minutes after treatment with antimycin A (20 μM, black bars) in nociceptive and non-nociceptive bronchopulmonary C-fibers, as defined by sensitivity to TRPV1 agonist (capsaicin, 1 μM) and conduction velocity (Kollarik et al., 2003). * Significant difference in mechanical sensitivity after antimycin A ($p<0.005$).

Fig 2. **Antimycin A increases α,β mATP-induced responses in nociceptive C-fibers.** A, representative traces of action potential discharge evoked by 10s challenge with α,β mATP ($P2X_{2/3}$ agonist, 30 μM) in a nociceptive bronchopulmonary C-fiber before (control) and 10 minutes after treatment with antimycin A (20 μM). Quantification of action potential discharge is shown below each trace. B, mean ± SEM total action potential discharge evoked by α,β mATP (30 μM) before (control, hatched bars) and 10 minutes after treatment with either vehicle (white bar) or antimycin A (20 μM, black bars) in nociceptive and non-nociceptive bronchopulmonary C-fibers. * Significant difference in 2^{nd} α,β mATP-induced responses after antimycin A ($p<0.01$). C, mean ± SEM peak action potential discharge evoked by α,β mATP (30 μM) before (control,

Molecular Pharmacology Fast Forward. Published on March 18, 2014 as DOI: 10.1124/mol.113.091272
This article has not been copyedited and formatted. The final version may differ from this version.

hatched bars) and 10 minutes after treatment with either vehicle (white bar) or antimycin A (20 μM, black bars) in nociceptive and non-nociceptive bronchopulmonary C-fibers. * Significant difference in 2nd α,β mATP-induced responses after antimycin A ($p<0.01$).

Fig 3. **Antimycin A-induced nociceptor hyperexcitability to α,β mATP is independent of TRPA1 and TRPV1.** A, mean ± SEM response to 2nd application of α,β mATP (30 μM) normalized to response to 1st application of α,β mATP prior to antimycin A (20 μM). Bronchopulmonary C-fibers were characterized by conduction velocity and sensitivity to TRPV1 agonist (capsaicin, 1 μM) and TRPA1 agonist (AITC, 300 μM) (Kollarik et al., 2003; Nassenstein et al., 2008). * Significant increase in 2nd α,β mATP-induced responses after antimycin A ($p<0.05$). B, mean ± SEM response to 2nd application of α,β mATP (30 μM) normalized to response to 1st application of α,β mATP prior to either vehicle (white bar) or antimycin A (20 μM, black bars) in nociceptive C-fibers. The role of TRPV1 in hyperexcitability was determined using pretreatment with the selective TRPV1 antagonist iodoresiniferatoxin (IRTX, 1 μM) or by using C-fibers from TRPV1-/- mice. * Significant increase in 2nd α,β mATP-induced responses after antimycin A compared to vehicle ($p<0.05$).

Fig 4. **Antimycin A-induced nociceptor hyperexcitability to α,β mATP is dependent on mitochondrial ROS and PKC.** A, mean ± SEM response to 2nd application of α,β mATP (30 μM) normalized to response to 1st application of α,β mATP prior to either vehicle (white bar), antimycin A (20 μM, black bar), oligomycin (10 μM, dark grey bar) or myxothiazol (500 nM, light grey bar) in nociceptive C-fibers. * Significant increase in 2nd α,β mATP-induced responses compared to vehicle ($p<0.01$). B, mean ± SEM response to 2nd application of α,β mATP (30 μM) normalized to response to 1st application of α,β mATP prior to either vehicle (white bar) or antimycin A (20 μM, black bars) in nociceptive C-fibers. The roles of ROS and PKC in

Molecular Pharmacology Fast Forward. Published on March 18, 2014 as DOI: 10.1124/mol.113.091272
This article has not been copyedited and formatted. The final version may differ from this version.

hyperexcitability to α,β mATP were determined using pretreatment with DTT (1mM), NAC (1mM), GSH (1mM), myxothiazol (500 nM), BIM I (1 μM) or BIM V (1 μM). * Significant increase in 2nd α,β mATP-induced responses after antimycin A compared to vehicle ($p<0.05$). # Significant reduction in antimycin A-induced hyperexcitability to α,β mATP ($p<0.05$).

Fig 5. **H_2O_2 increases α,β mATP-induced responses in nociceptive C-fibers via PKC.** A, mean ± SEM response to 2nd application of α,β mATP (30 μM) normalized to response to 1st application of α,β mATP prior to either vehicle (white bar), PMA (3 μM, grey bar), or H_2O_2 (1 mM, black bars) in nociceptive C-fibers. The roles of PKC in H_2O_2-induced hyperexcitability to α,β mATP were determined using pretreatment with BIM I (1 μM). * Significant increase in 2nd α,β mATP-induced responses compared to vehicle ($p<0.05$). # Significant reduction in H_2O_2-induced hyperexcitability to α,β mATP ($p<0.005$).

Fig 6. **Antimycin A induces PKC translocation to the plasma membrane via ROS in vagal neurons.** A-E, representative confocal images of PKC (red) and nuclei (DAPI blue) in dissociated vagal sensory neurons. Scale denotes 25 μm. In dissociated ganglia preparations neurons are typically >20 μm in diameter; other non-neuronal cell types are also present which are small with substantial nuclei (Nassenstein et al., 2010). A, control conditions. B, after PMA (300nM). C, after antimycin A (10 μM). D, after antimycin A (10 μM) pretreatment with tempol (1mM) and MnTMPyP (50 μM). E, after H_2O_2 (300 μM). F, mean ± SEM PKC membrane/cytosolic ratio for experiments described in A-E. * Significant increase in membrane/cytosolic ratio compared to vehicle ($p<0.005$). # Significant reduction in membrane/cytosolic ratio compared to antimycin A alone ($p<0.05$).

Figure 1

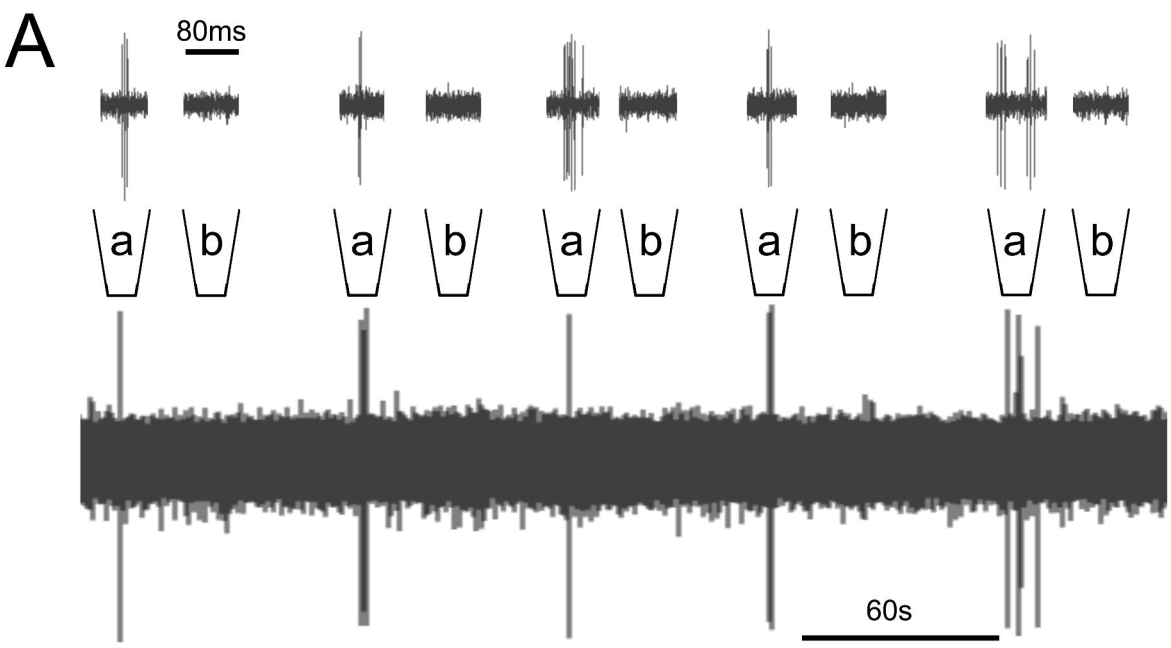

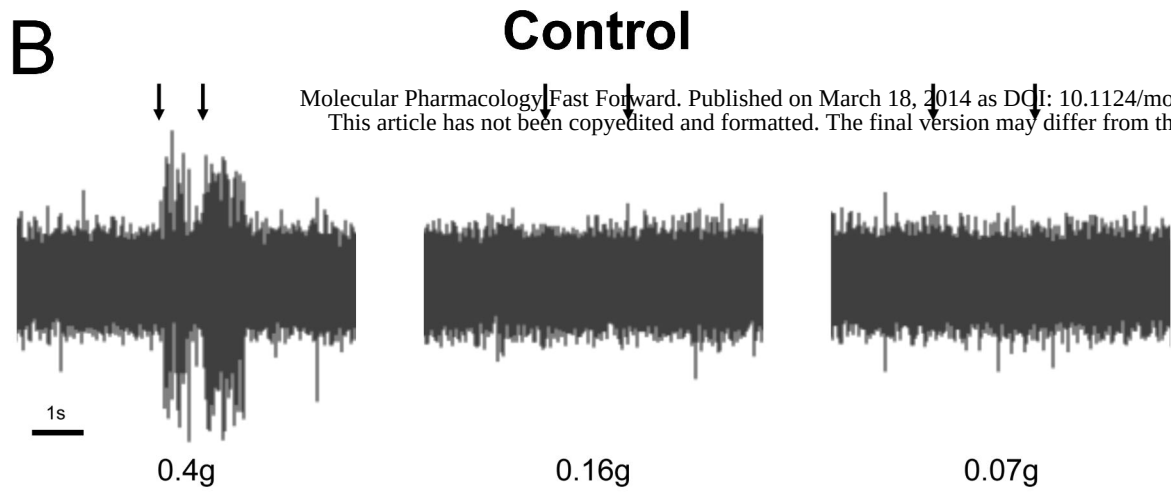

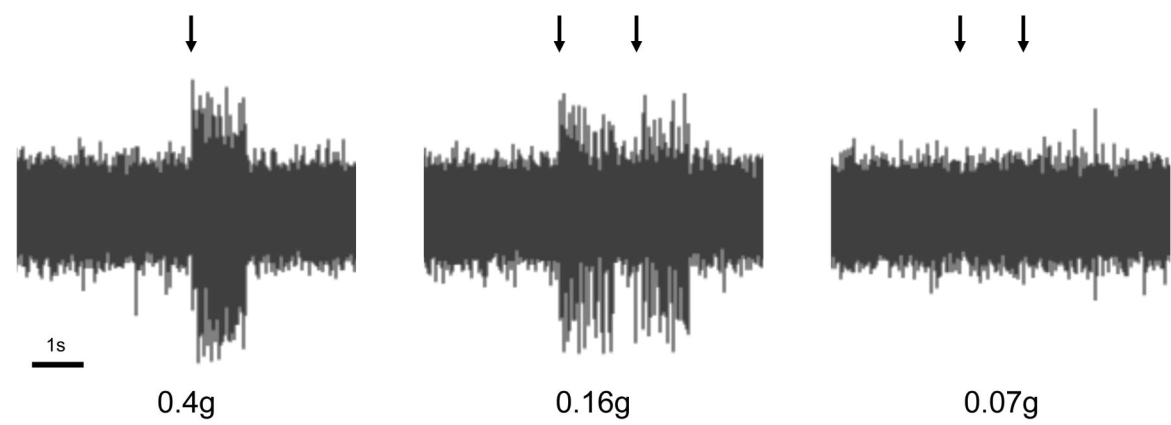

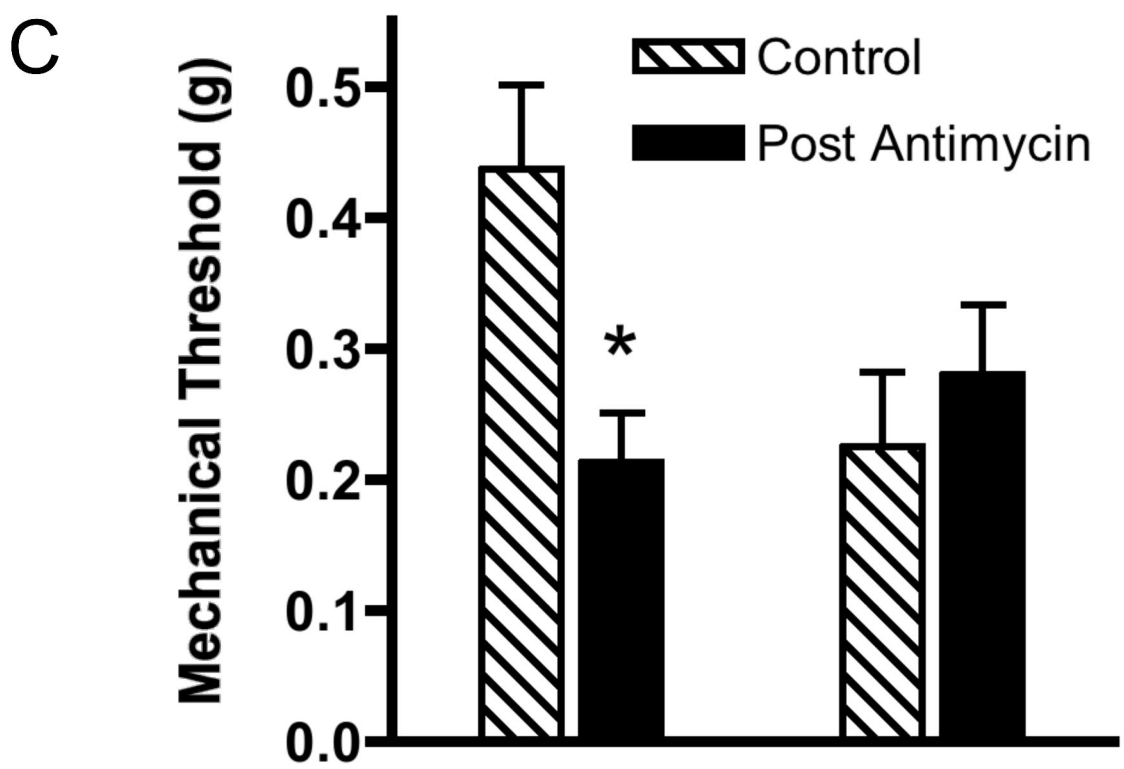

Sensitive to TRPV1 agonist	+	-
Nociceptor?	**Yes**	No
CV (m/s)	0.56 (±0.04)	1.01 (±0.40)

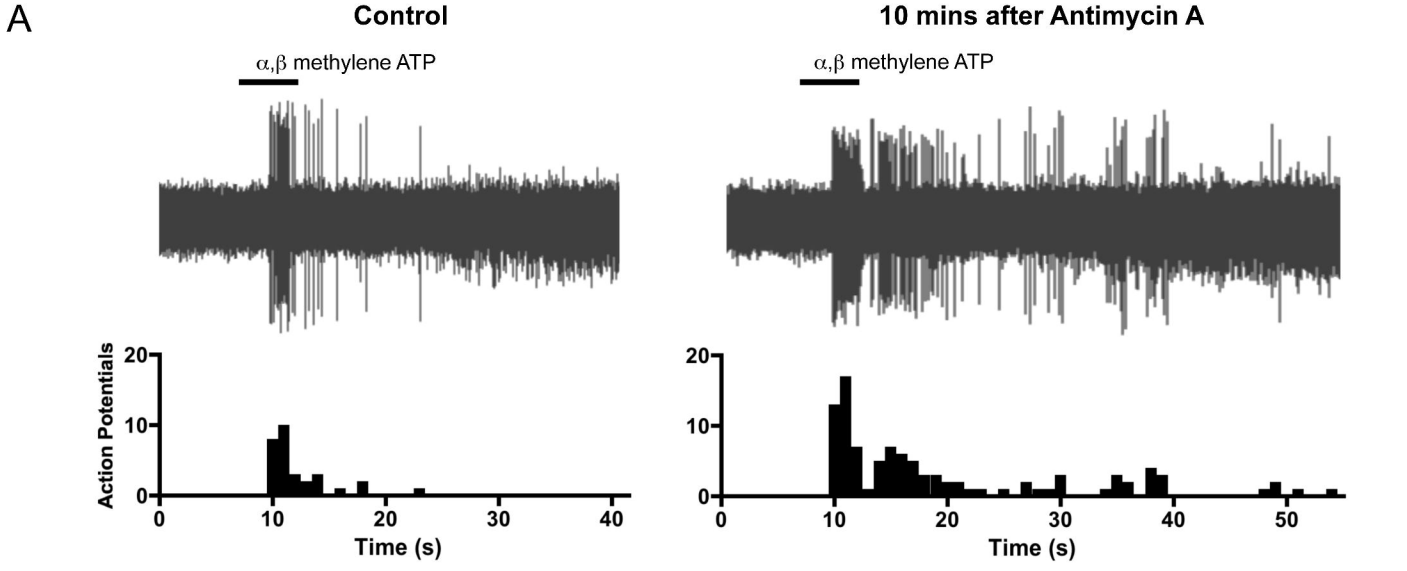

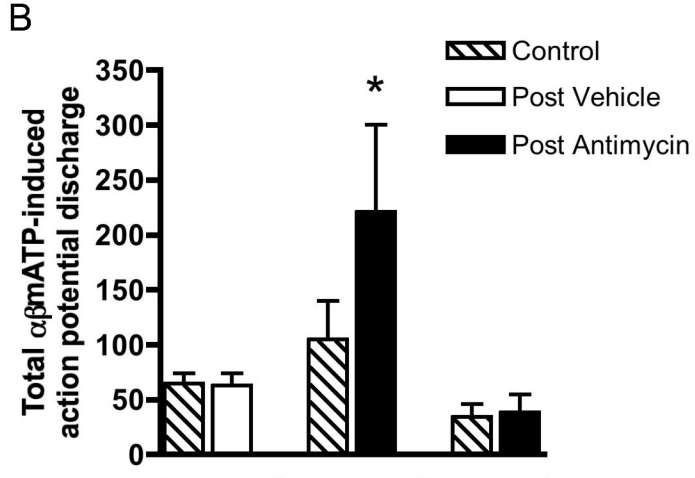

Sensitive to TRPV1 agonist	+	+	-
Nociceptor?	**Yes**	**Yes**	No
CV (m/s)	0.51 (±0.02)	0.56 (±0.02)	1.01 (±0.40)

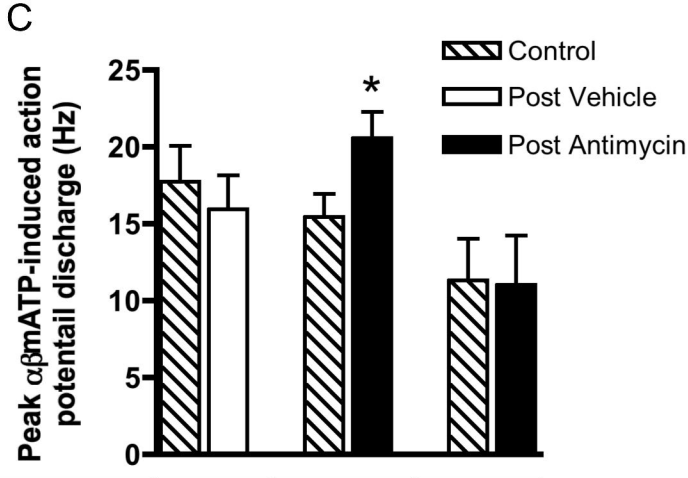

Sensitive to TRPV1 agonist	+	+	-
Nociceptor?	**Yes**	**Yes**	No
CV (m/s)	0.51 (±0.02)	0.56 (±0.02)	1.01 (±0.40)

Figure 2

Figure 3

A

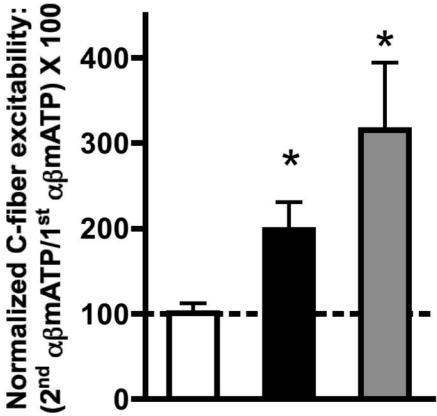

Sensitive to TRPA1 agonist	-	+	-
Sensitive to TRPV1 agonist	-	+	+
Nociceptor?	No	**Yes**	**Yes**
CV (m/s)	1.01 (±0.40)	0.56 (±0.05)	0.56 (±0.02)

B

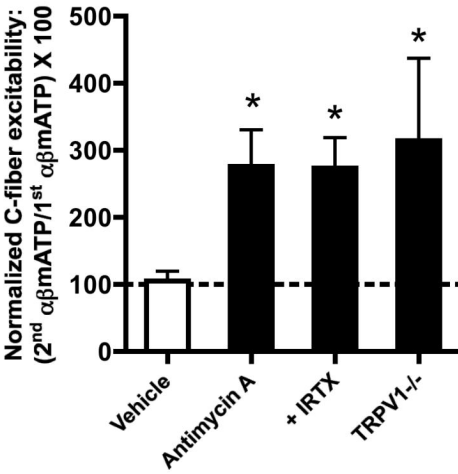

Figure 4

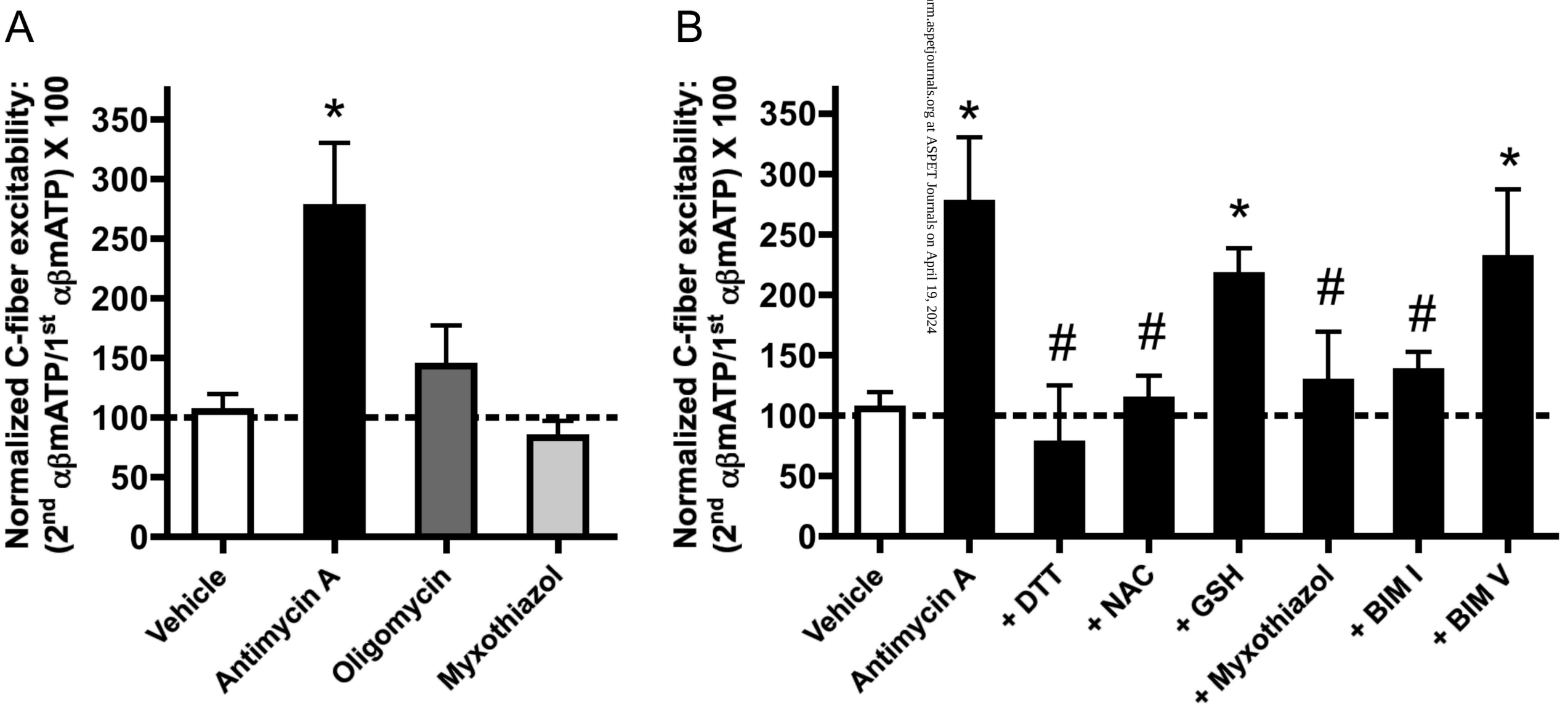

Figure 5

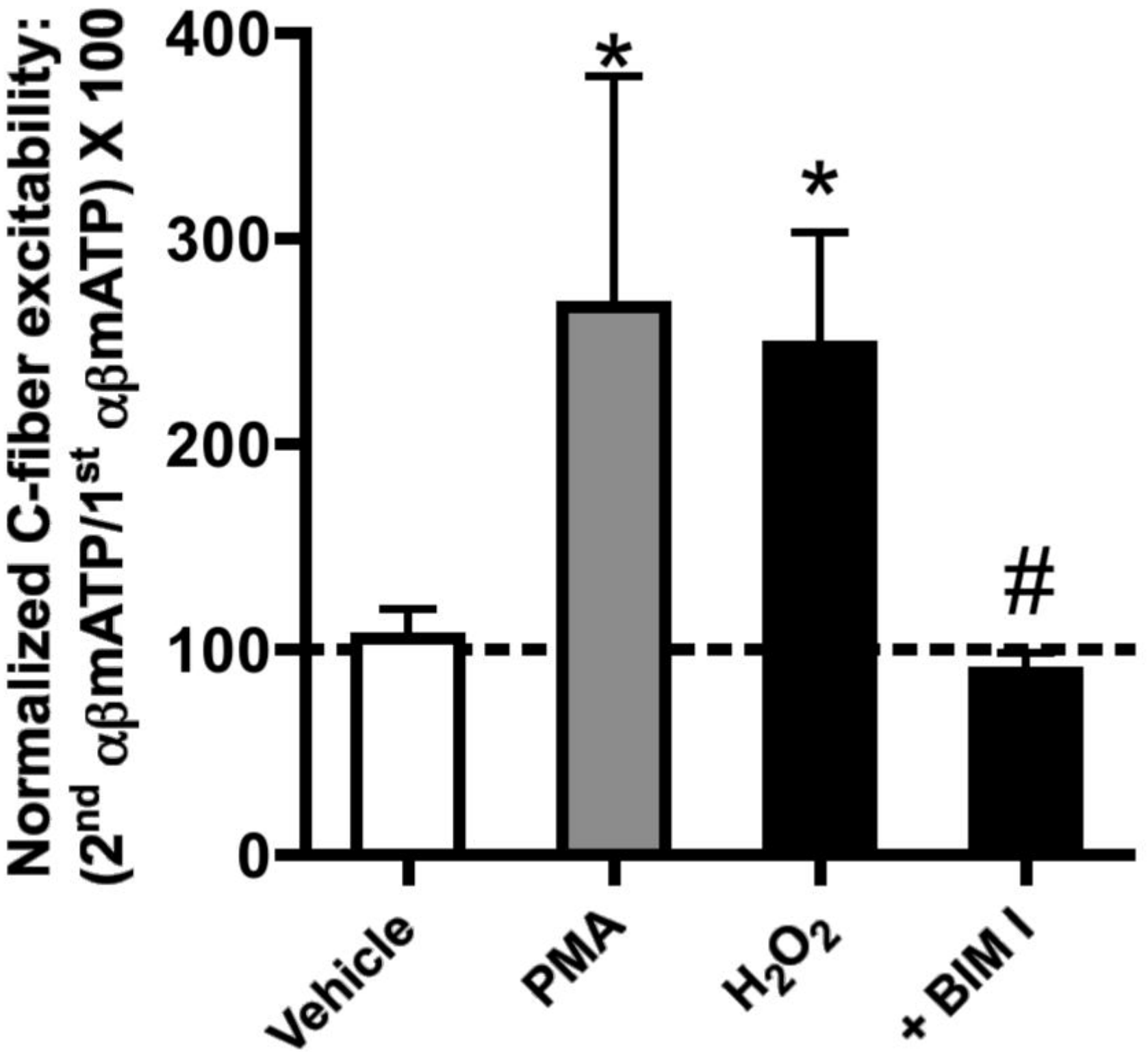
Normalized C-fiber excitability:
(2nd αβmATP/1st αβmATP) X 100
400
300
200
100
0
*
*
#
Vehicle
PMA
H2O2
+ BIM I

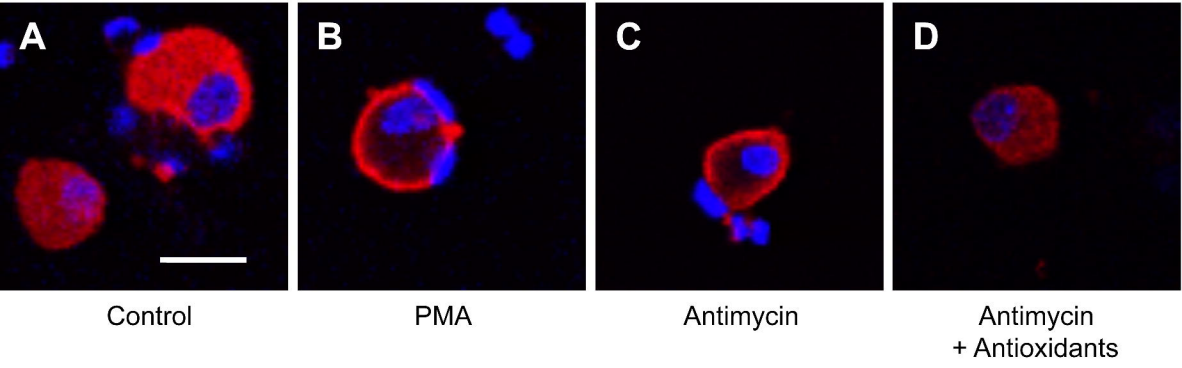
A
B
C
D
Control
PMA
Antimycin
Antimycin
+ Antioxidants

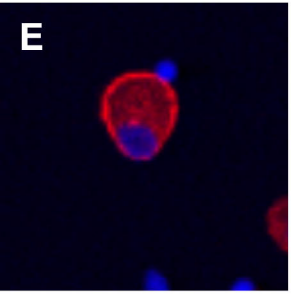
E
H_2O_2

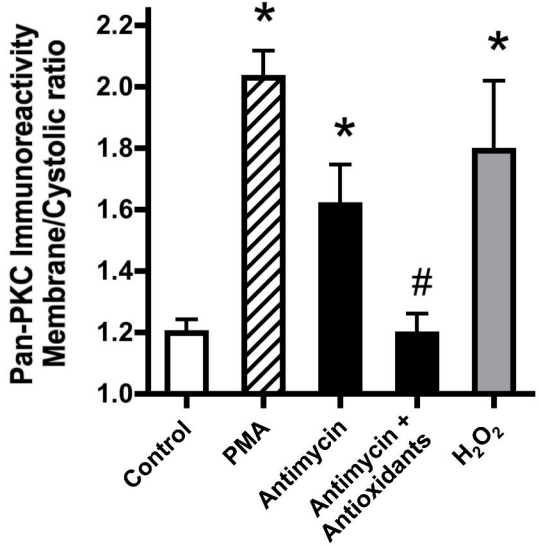
F
Pan-PKC Immunoreactivity
Membrane/Cystolic ratio
2.2
2.0
1.8
1.6
1.4
1.2
1.0
*
*
#
*
Control
PMA
Antimycin
Antimycin +
Antioxidants
H_2O_2

Figure 6